2019 IMEKO TC-19 International Workshop on
Metrology for the Sea
Genoa, Italy, October 3-5, 2019

Testing a GNSS software receiver for end-user utilization

Matteo Cutugno[1], Umberto Robustelli[2], Giovanni Pugliano[3]

[1]*Department of Engineering, Parthenope University of Naples, 80133 Naples, Italy; E-mail: matteo.cutugno@uniparthenope.it*
[2]*Department of Engineering, Parthenope University of Naples, 80133 Naples, Italy; E-mail: umberto.robustelli@uniparthenope.it*
[3] *Department of Engineering, Parthenope University of Naples, 80133 Naples, Italy; E-mail: giovanni.pugliano@uniparthenope.it*

***Abstract* – Software Defined Receivers(SDR) can be a very useful tools both for researchers and surveyors since it is capable of extreme customization allowing user to access, visualize and modify signal processing blocks. In this paper we test the single point performance of the GNSS-SDR software receiver coupled with Nuand BladeRF x40 front-end feeded by an active u-blox GNSS antenna powered by a bias-tee needful to provide external gain. Four different tests have been carried out in two different scenarios located in Naples (Italy) employing two different antennas: the first dataset was acquired in a site expected to be a low-multipath environment while the second in a strong multipath scenario in Centro Direzionale (CDN) site using the same instrumentation. Both tests were carried out with two different antennas. Results achieved show how SDR is a good candidate to represent an innovative low-cost and flexible platform which can be used to get intermediate frequency data useful in the field of GNSS reflectometry and ionospheric scintillation analysis.**

I. INTRODUCTION

The satellite navigation scenario has observed the advent of a number of new systems and technologies: after the landmark design and development of the Global Positioning System (GPS), a number of new Global Navigation Satellite Systems (GNSSs) were or are being developed all over the world: Russia's GLONASS, Europe's GALILEO, and China's BEIDOU2. With such a quickly improving of the GNSS scenario the future receivers must be able to take advantages of these potentials. In this perspective Software Defined Receivers (SDR) can be very useful tools both for researchers and surveyors. In fact, despite commercial receivers can assure great performance, they are a black box preventing user to access algorithms involved in positioning process and, often, limiting the possibilities of upgrading. On the other hand, SDR is capable of extreme customization allowing user to access, visualize and modify signal processing blocks. SDR refers to an ensemble of hardware and software technologies and design choices that allow re-configurable radio communication architectures. The main idea behind this concept is to replace the dedicated hardware components by means of software modules. The most common architecture of a GNSS SDR receiver is shown in Figure 1. The following operations are performed by the processing chain:

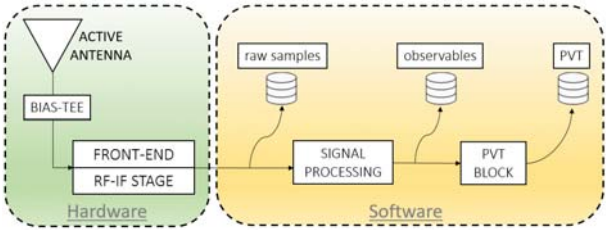

Figure 1: General SDR Architecture

- the signal captured by the GNSS antenna is demodulated at an Intermediate Frequency (IF), sampled and quantized by the Radio Frequency front-end. The latter, which acts as data grabber, streams digital raw samples as output.
- the samples are then fed to the signal processing stage which can process the stored data either in real time or in a post-processing stage giving as output the observables by means of post correlation data.
- the last block performs the positioning algorithms by computing the Position, Velocity and Time solutions (PVT).

Nowadays there are some software solutions in GNSS positiong following this approach: PLAN research group from Calgary University in 2008 propose GSNRx (GNSS software navigation receiver) [1] where the SDR is tested and showed accuracy to the meter level, as expected given the low level of ionospheric activity during the test and the relatively benign multipath environment in which the data was collected; Munich University create in 2007 ipexSR presented in [2] where some indoor tests are performed

showing a position accuracy level of better than 20 meters; furthermore, ISMB in collaboration with Politechnic University of Turin propose in 2009 N-Gene where in [3] are presented the solutions adopted for the signal acquisition and tracking tested. According to [4], a number of commercially successful GNSS receivers were developed combining dedicated system-on-chip architecture and many of the benefits provided by software-defined radio, including Swift Navigation Piksi Multi GNSS Module1[5]. Earlier SDR concept was applied in low-cost dual-frequency GPS receiver CASES presented in [6] and designed for ionosphere monitoring. The most well-known practical ready-to-use implementation of SDR in GNSS is Trimble Catalyst [7]. Surveying grade GNSS antenna module (RF front-end) is connected via USB port to a smartphone or tablet computer with installed software-defined GNSS receiver. However, the most promising software receiver capable to acquire, process and compute navigation solution for different constellations (GPS, Glonass and Galileo) seems to be GNSS-SDR [8] developed by CTTC (Centre Tecnologic Telecomunicacions Catalunya). In this paper the choice has fallen on this last software for all sorts of things. First of all, it is released on General Public License offering a full customization thanks to the open source code freely available; the open source project, hosted on github.com can rely on a very active community of developers. Furthermore, it allows to work with a lot of low-cost front ends offering for each of this hardware the libraries needed to build the interface software-hardware. The main objective of this paper is the evaluation of Nuand BladeRF x40 performance in the single point positioning domain for L1 GPS signal. Figure 1 shows a general SDR architecture made up of a front-end connected to an active antenna feeded by a bias-tee, delivering digital signal samples to successive processing stage in a processing unit environment.

II. METODOLOGY

The methodology used to achieve single point positioning with GNSS pseudoranges is well known and widely described in [9]. However, a brief recall is provided here to describe the algorithms used to implement the software developed. GNSS receivers provide four types of measurements for each frequency: pseudorange, Doppler, carrier phase and carrier-to-noise. The first three measurements are used to achieve receiver position [10] while the carrier-to-noise density provides an indication of the accuracy of the tracked GNSS satellite observations and the noise density as seen by the receiver's front-end [11]. It also indicates the level of noise present in the measurements. To achieve the receiver coordinates and offset, at least four equations are necessary; they can be linearized around an a priori unknown estimation obtaining:

$$\underline{\Delta\rho} = H \cdot \underline{\Delta X} + \underline{\epsilon} \tag{1}$$

where:
$\Delta\rho$ $(nx1)$ is the difference vector between the n raw pseudoranges and a priori information (with n number of Gps observations),
H is (n x 4) design matrix,
ΔX (4 x 1) is the state vector,
ϵ is the residuals vector which includes all unmodelled errors (measurement noise, multipath and so on).
The explicit forms of H and ΔX are:

$$H = \begin{bmatrix} \frac{X_0 - X^{G1}}{\rho_0^{G1}} & \frac{Y_0 - Y^{G1}}{\rho_0^{G1}} & \frac{Z_0 - Z^{G1}}{\rho_0^{G1}} & 1 \\ \frac{X_0 - X^{G2}}{\rho_0^{G2}} & \frac{Y_0 - Y^{G2}}{\rho_0^{G2}} & \frac{Z_0 - Z^{G2}}{\rho_0^{G2}} & 1 \\ \vdots & \vdots & \vdots & \vdots \\ \frac{X_0 - X^{Gi}}{\rho_0^{Gi}} & \frac{Y_0 - Y^{Gi}}{\rho_0^{Gi}} & \frac{Z_0 - Z^{Gi}}{\rho_0^{Gi}} & 1 \\ \vdots & \vdots & \vdots & \vdots \\ \frac{X_0 - X^{Gn}}{\rho_0^{Gn}} & \frac{Y_0 - Y^{Gn}}{\rho_0^{Gn}} & \frac{Z_0 - Z^{Gn}}{\rho_0^{Gn}} & 1 \end{bmatrix}$$

$$\underline{\Delta X} = \begin{bmatrix} \Delta X & \Delta Y & \Delta Z & \Delta(c\delta T_{RX}) \end{bmatrix}$$

where the superscript n is the number of GPS simultaneous measurements and $\rho_0^G n$ is the a priori pseudorange of n Gps satellite. The set of equation 1 is solved for ΔX by means of Weighted Least Square (WLS) method and the solution is given by the equation:

$$\underline{\Delta X} = (H^T W H)^{-1} \cdot H^T W \Delta\rho \tag{2}$$

where: W *(nxn)* is the weighting matrix. It can be set as the inverse of the measurement covariance matrix R, weighting the accurate measurements more and the noisy ones less. Here all pseudorange errors are considered independent thus covariance matrix is set equal to identity matrix with the weights calculated as function of the satellite elevation angle.

$$W = R^{-1} \textit{diag(weight)}, \tag{3}$$

The LS estimation is used to update the a priori value:

$$\underline{\hat{X}} = \underline{X_0} + \Delta\underline{X}, \tag{4}$$

In the scenario of simultaneous employment of Galileo and GPS constellations the expression of matrix H and vector ΔX are reported in [12] while a deep analysis of Galileo code measurements has been performed in [13].

III. EXPERIMENTAL SETUP

A. *Hardware setup*

With reference to Figure 1, inside the green box is shown the minimum hardware needed for SDR; in particular the configuration consisted in: a front-end, a bias-tee, an active antenna and a notebook. The front-end tested in this paper is a Nuand bladeRF x40, a low-cost USB 3.0 Software Defined Radio, able to tune up from 300MHz to 3.8GHz; so,

potentially, it can provide access to all of the frequency used by GNSS satellites (L1, L2 and L5). Its price is about $400. This board is equipped with a Field Programmable Gate Array (FPGA) that provides the interface between the firmware and RF transceiver. This FPGA has single-cycle access embedded memory, hard 18x18 multipliers for dedicated DSP and many general logic elements ready to be programmed. In order to evaluate this board for GNSS positioning, for this first application we just use it in single frequency (L1). The front-end has been connected to a notebook via USB 3.0. The notebook is equipped with a intel i7 microprocessor with 16 Gb of RAM running a stable release of Ubuntu 16.04. The hardware needed was completed by a low-cost GNSS antenna and a bias-tee. Two different antennas were tested. In Table 1 are shown the main features of the active u-blox GNSS antennas employed. As previously said these antennas were low-cost ones where the latter being more expensive shows better performances respect to the former. Lastly, the hardware configuration was completed by a bias-tee, needful to provide external gain to the antenna, feeded by 5 volt provided via a USB port.

	ANN-MS L1 band	ANN-MB L1 band
Frequency [MHz]	1555 - 1605	1559 - 1606
Impedance [Ohm]	50	50
Peak gain [dBic]	Min.4	Typ.3.5
Gain(no cable)[dB]	29	25 - 31
Noise figure [dB]	0.9	2.8
DC voltage [V]	2.7 - 5.5	3 - 5
Polarization	RHCP	RHCP
Price [€]	15	55

Table 1: Antennas characteristics.

B. Software setup

Referring to Figure 1 the yellow box represents the whole signal processing tasks running on the processing unit by means of the software. As previously said the software chosen for this tests is GNSS-SDR, an open source project hosted on *github.com* that implements a complete global navigation satellite system software defined receiver in C++. It performs signal acquisition and tracking of the available satellite signals, decodes the navigation message and computes the observables needed by positioning algorithms, which ultimately compute the navigation solution. In this experiment we set up SDR to store Intermediate Frequency (IF) signal. The data storage requirement depends on the received signal bands and number of bits used to represent each digital sample [14]. In particular, we experienced that the space needed to store raw data for L1 frequency packed in complex samples, with real and imaginary parts of type float, was $\sim$ 1 GB for every minute of acquired data. After the acquisition step IF data were post-processed in order to achieve pseudorange measurements lastly used to compute single point position solution.

Figure 2: Acquisition scenarios: Eremo site on the left; CDN site on the right.

C. Acquisition Scenarios

In order to investigate the performance of the hardware involved we applied our analysis to the measurements captured in two different scenarios where we tested two different low-cost antennas. The first dataset was acquired in a site expected to be a low-multipath environment. The receiver was placed in Eremo site (Naples, Italy) as shown in Figure 2. The experiment was carried out on the 8th of May 2019 acquiring thirty minutes of raw data corresponding to about 30 GB of storage. The second dataset was collected on the 10th of July 2019 for the same duration in a strong multipath scenario in Centro Direzionale (CDN) site (Naples, Italy) using the same instrumentation. From Figure 2 one ca notice that this is a difficult environment in which the receivers are surrounded by buildings. It can be seen as a typical example of an urban canyon where many GNSS signals are strongly degraded by multipath effects or blocked by skyscrapers. The analysis was performed for all visible satellites of GPS and Galileo constellations for all of the four experiments during the whole observation periods. In order to evaluate the performance of the software receiver, we used as term of comparison the TOPCON GRS-1 geodetic receiver fed by the geodetic dual frequency (L1/L2) dual constellation (GPS/GLONASS) TOPCON PG-A1 antenna. So, for sake of clarity the features of the tests conducted in this paper are shown in Table 2.

	Site	Antenna	n° of obs
Test 1	Eremo	ANN-MS	453
Test 2	CDN	ANN-MS	258
Test 3	Eremo	ANN-MB	4629
Test 4	CDN	ANN-MB	3599

Table 2: Tests conducted.

IV. PRELIMINARY RESULTS

In order to assess the quality of the generated pseudorange measurements the carrier-to-noise density C/N_0 output was analyzed and compared to that of the geodetic receiver only for GPS constellation. As well-known, C/N_0

provides an indication of the accuracy of the tracked satellite observations, the noise density as seen by the receiver's front-end and multipath error. The lower the signal-to-noise ratio the worse the quality of the measurements. Figure 3 shows a comparison of the mean of C/N_0 values for each tracked satellite in Eremo sites for SDR and Geodetic receiver. As expected SDR tracks less satellites than geodetic receiver. Moreover the C/N_0 values for SDR are lower respect to those of geodetic receiver due, probably, to the fact that the u-blox antennas are low cost hardware compared to the geodetic one. In addiction, in Figure 4

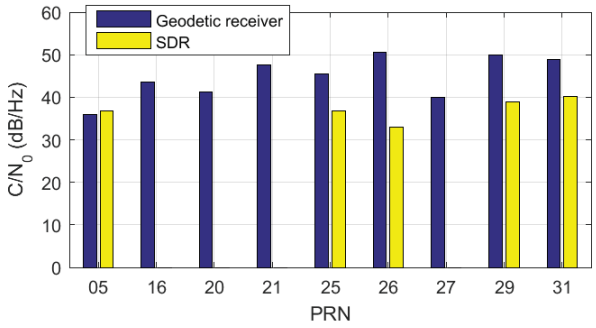

Figure 3: Signal Noise Ratio mean of Geodetic and SD receivers for Eremo site.

are shown the skyplots for Eremo and CDN sites. As noticed in this Figure the skyplots on the left, representing the Eremo scenario show the capability of SDR to acquire also Galileo satellites while this capability fails in the CDN scenario. Figure 6 shows the scatter plots obtained

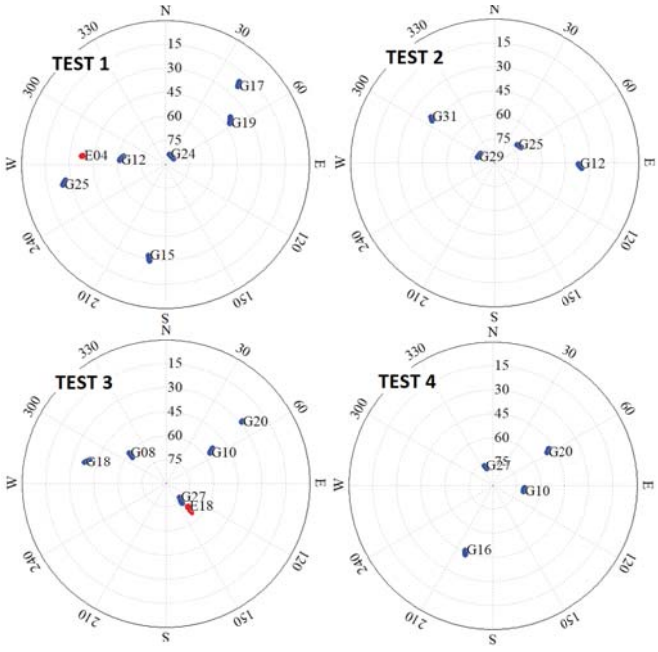

Figure 4: Skyplots for all tests conducted.

by processing pseudorange measurements for the four test conducted. It can be noted that the computed solutions

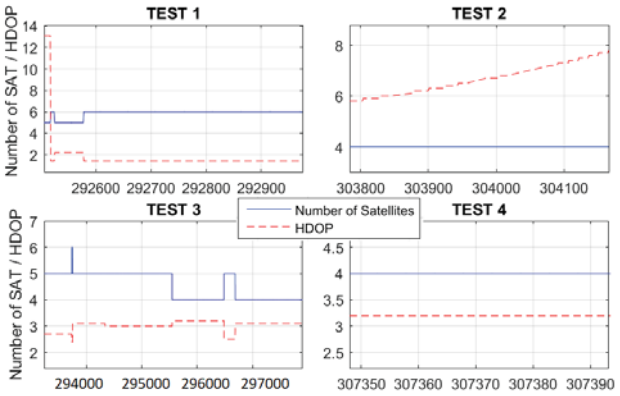

Figure 5: Number of Satellites and HDOP for all tests conducted.

obtained with the ANN-MS antenna are worst respect to those of Eremo. In particular the length of the acquisition step and then the number of computed solution are abundant with ANN-MB antenna respect to the other ones. The reason can be found in the fact that the better antenna shows higher Carrier to noise density ratio (C/N_0) assuring a stronger and more reliable tracking process yielding to a more stable computing stage. Infact, analysing the output of the processed data, we found that the mean value of C/N_0 for the ANN-MB antenna is almost 2 dB-Hz greater than the same parameter of ANN-MS antenna. Furthermore, Figure 5 asses satellites availability showing the number of satellites and Horizontal Diluition Of Precision (HDOP); this Figure reveals suitable values of HDOP for Test 1 and Test 3, whereas this parameter degrades for Test 2 and Test 4. However, both measurements revealed a good position accuracy; in fact, the mean values of the position solutions in Eremo site (Test 1 and Test 3) differs respect to those of geodetic receiver by 0.54 meters for the East component, by 1.41 meters for the North component and by 5.46 meters for the Up component with the ANN-MS antenna, whereas with the better one those mean values are 0.27 meters for the East component, 4.84 meters for the North component and 9.63 meters for the Up component. On the other hand, in CDN site (Test 2 and Test 4), the accuracy has degraded; in fact, referring to Test 2 the mean values of the position solutions differs respect to those of geodetic receiver by 2.09 meters for the East component, by 4.84 meters for the North component and by 9.63 meters for the Up component while Test 4 shows a difference of position solution of 0.66 meters for the East component, 1.96 meters for the North component and, lastly, 6.01 meters for the Up component. Figure 7 and Figure 8 show North, East and Up error components with the ANN-MS antenna for Eremo and CDN sites, respectively. The comparison of these figures highlights a strong dispersion of position solutions for the North component in CDN site, with respect to those in Eremo site, as expected. Fig-

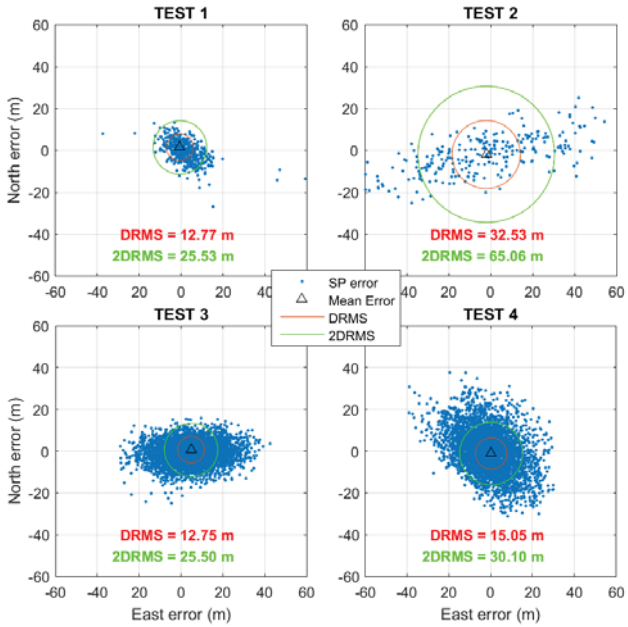

Figure 6: Scatter plot of L1 single point position errors for Eremo (Test 1 and Test 3) and CDN (Test 2 and Test 4).

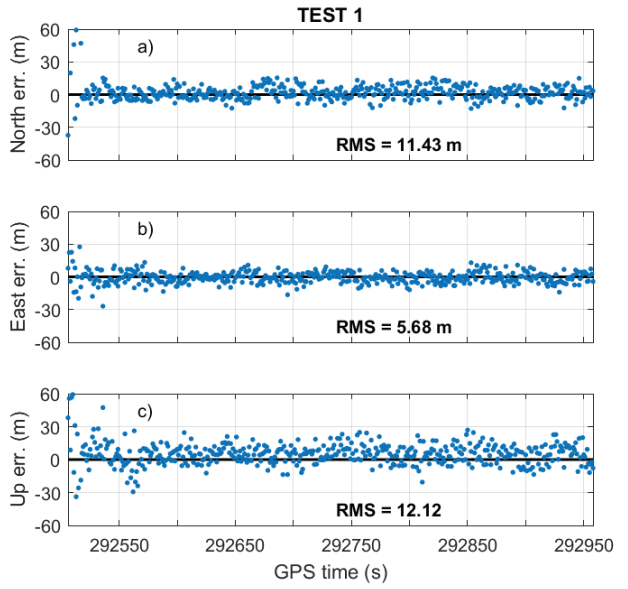

Figure 7: Single point positioning solution for Eremo site employing the ANN-MS antenna, in a) b) and c) are shown North, East and Up errors respectively

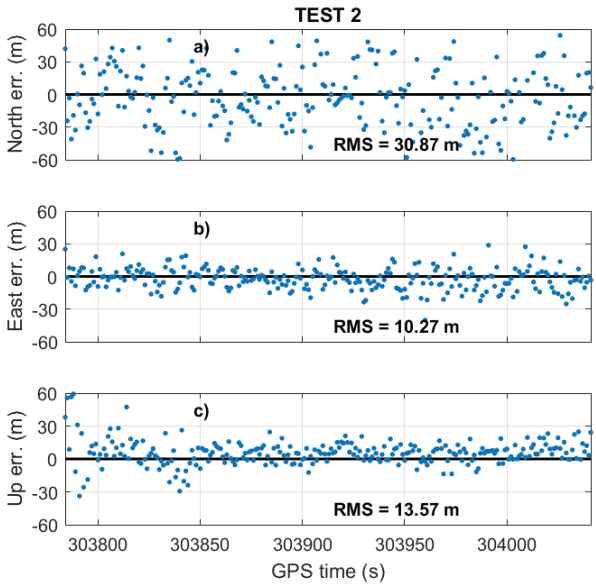

Figure 8: Single point positioning solution for CDN site employing the ANN-MS antenna, in a) b) and c) are shown North, East and Up errors respectively

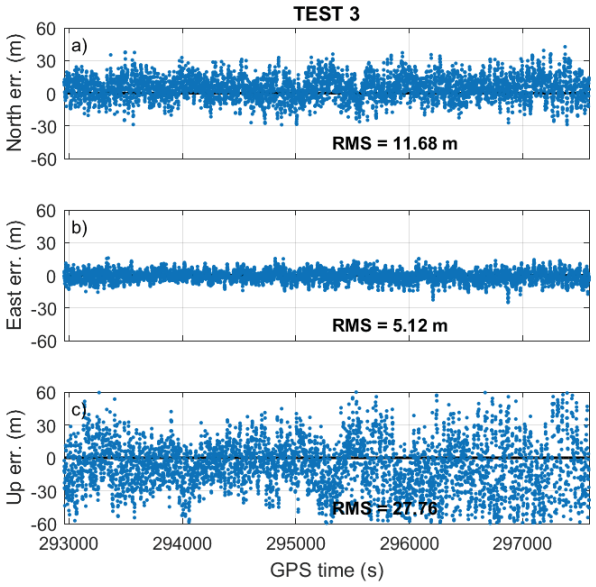

Figure 9: Single point positioning solution for Eremo site employing the ANN-MB antenna, in a) b) and c) are shown North, East and Up errors respectively

ure 9 and Figure 10 show North, East and Up error components with the ANN-MB antenna for Eremo and CDN sites, respectively. In Table 3 the statistics of the single-point positioning analysis are summarized. The horizontal position error in CDN site is two times and half the value of Eremo site. This was an expected result bearing in mind that the two scenarios are very different one from another in terms of satellites visibility and multipath error. Moreover the values of RMS in Test 3 and Test 4, strongly decrease.Comparable results, tough obtained with L2 frequency, are reported in [15].

V. CONCLUSIONS

The performance assessment in the domain of single point positioning of low-cost front-end, based on a SDR technology, has been presented. Results achieved are as good as those obtainable by traditional low-cost hardware receiver. The most interesting feature of this approach is

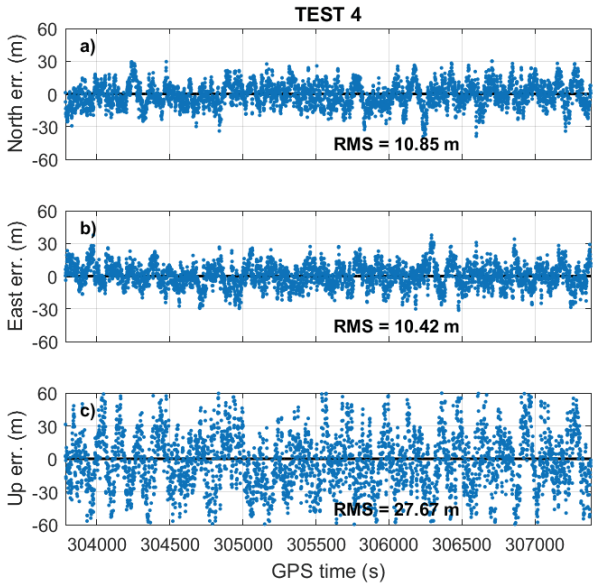

Figure 10: Single point positioning solution for CDN site employing the ANN-MB antenna, in a) b) and c) are shown North, East and Up errors respectively

	RMS East [m]	RMS North [m]	RMS Up [m]	2D RMS [m]
Test 1	5.68	11.69	12.12	12.77
Test 2	10.27	30.84	13.57	32.53
Test 3	5.12	11.43	27.76	12.75
Test 4	10.42	10.85	27.67	15.05

Table 3: Summary table of the performance of single-point positioning for all the tests conducted.

the possibility to store intermediate output at different levels of processing stages in order to analyse raw data such as Intermediate Frequency signal and observables measurements. The future work planned consist in taking advantage of this technology. In fact, software defined receivers can be good candidates to represent an innovative low-cost and flexible platforms for multipath error studies, ionospheric scintillation analysis and, above all, GNSS Reflectometry test and development. The test analysis carried out shows that the employment of a more performing antenna gives better results for single point positioning solutions.

VI. REFERENCES

[1] M. Petovello, C. O'Driscoll, G. Lachapelle, D. Borio, and H. Murtaza, "Architecture and Benefits of an Advanced GNSS Software Receiver," Positioning, vol. 1, pp. 66–78, 12 2008.

[2] M. Anghileri, T. Pany, D. S. Güixens, J.-H. Won, A. Sicramaz Ayaz, C. Stöber, I. Krämer, D. Dötterböck, G. Hein, and B. Eissfeller, "Performance Evaluation of a Multi–frequency GPS/Galileo/SBAS Software Receiver," proc. of ION GNSS'07, pp. 2749–2761, 01 2001.

[3] M. Fantino, A. Molino, and M. Nicola, "N–Gene GNSS Receiver: Benefits of Software Radio in Navigation," proc. of ENC-GNSS'09, 05 2009.

[4] A. M. James T. Curran, Carles Fernández-Prades and M. Bavaro, "Innovation: The continued evolution of the GNSS software-defined radio," GPS world, January 2018.

[5] "Piksi High Precision GPS, GNSS, Centimeter-level relative positioning." `https://www.swiftnav.com/piksi-multi`. Accessed: 2019-08-30.

[6] G. Crowley, G. Bust, A. Reynolds, S. Azeem, R. Wilder, B. Ńanlon, M. Psiaki, S. Powell, T. Humphreys, and J. Bhatti, "CASES: A novel low-cost ground-based dual–frequency GPS software receiver and space weather monitor," 24th International Technical Meeting of the Satellite Division of the Institute of Navigation 2011, ION GNSS 2011, vol. 2, pp. 1437–1446, 01 2011.

[7] "Trimble Catalyst." `https://geospatial.trimble.com/catalyst`. Accessed: 2019-08-30.

[8] C. Fernández-Prades, J. Arribas, P. Closas, C. Avilés, and L. Esteve, "GNSS-SDR: An open source tool for researchers and developers," 24th, ION GNSS 2011, vol. 2, 09 2011.

[9] G. Strang and K. Borre, Linear Algebra, Geodesy, and GPS. Wellesley-Cambridge Press, 1997.

[10] U. Robustelli and G. Pugliano, "GNSS Code Multipath Short-time Fourier Transform Analysis," Navigation, vol. 65, no. 3, pp. 353–362, 2019.

[11] U. Robustelli, V. Baiocchi, and G. Pugliano, "Assessment of Dual Frequency GNSS Observations from a Xiaomi Mi 8 Android Smartphone and Positioning Performance Analysis," Electronics, vol. 8, January 2019.

[12] A. Angrisano, S. Gaglione, C. Gioia, U. Robustelli, and M. Vultaggio, "GIOVE Satellites Pseudorange Error Assessment," Journal of Navigation, vol. 65, no. 1, pp. 29–40, 2012.

[13] U. Robustelli and G. Pugliano, "Code multipath analysis of Galileo FOC satellites by time-frequency representation," Applied Geomatics, vol. 11, pp. 69–80, 2019.

[14] G. Lachapelle and A. Broumandan, "Benefits of GNSS IF data recording," proc. of ENC-GNSS'16, pp. 1–6, 05 2016.

[15] C. Fernández-Prades, J. Vilá-Valls, J. Arribas, and A. Ramos, "Continuous Reproducibility in GNSS Signal Processing," IEEE Access, pp. 20451–20463, 04 2018.